

# RSC Advances



This is an *Accepted Manuscript*, which has been through the Royal Society of Chemistry peer review process and has been accepted for publication.

*Accepted Manuscripts* are published online shortly after acceptance, before technical editing, formatting and proof reading. Using this free service, authors can make their results available to the community, in citable form, before we publish the edited article. This *Accepted Manuscript* will be replaced by the edited, formatted and paginated article as soon as this is available.

You can find more information about *Accepted Manuscripts* in the [Information for Authors](#).

Please note that technical editing may introduce minor changes to the text and/or graphics, which may alter content. The journal's standard [Terms & Conditions](#) and the [Ethical guidelines](#) still apply. In no event shall the Royal Society of Chemistry be held responsible for any errors or omissions in this *Accepted Manuscript* or any consequences arising from the use of any information it contains.

## ARTICLE

# Polymer Melts Flow through Nanochannels: from Theory, Fabrication to Application

Cite this: DOI: 10.1039/x0xx00000x

Sarmad Ali, Wei Tian\*, Nisar Ali, Lingxiao Shi, Jie Kong, Nazakat Ali

Received 00th January 2014,  
Accepted 00th January 2014

DOI: 10.1039/x0xx00000x

www.rsc.org/

Polymer nanotubes/nanorods have recently received much more interest and have become a magnetic topic in the interdisciplinary field of nanoscience and nanotechnology. Generally, they can be easily fabricated by template wetting of polymer melts. This short review presents effective ways to enhance polymer melts flow in nanochannels, typically focused on influencing wetting parameters including time, temperature, size of nanochannels and surface properties of the inner wall of nanochannels. Then, the investigation progress on polymer nanotubes/nanorods nanofabrication by nanoporous alumina template wetting was discussed. Many applications of polymer nanotubes/nanorods fabricated by template wetting from photonics to sensors and medical devices were summarized in the last section of this review.

## 1. Introduction

The behavior of liquids or melts flowing through nanochannels has been given great importance recently, especially with the emergence of micro/nano-fabrication processes based on polymer flow, the enhancement in flow and a reduction in intermolecular entanglements are of significant importance in the design and execution of processing methods. With the current progress in synthesis routes and emerging technologies, it is possible to reproducibly fabricate and study nanostructured polymer systems such as thin films, nanowires, nanotubes, nanoparticles, nanorods and nanoporous materials.<sup>1-3</sup>

To achieve the flow of polymer melts in nanochannels, it must be noticed as well as much necessary about the wetting phenomenon of liquid on a high-energy surface.<sup>4,5</sup> Owing to prepare nanochannels using solid materials with high surface energy, polymer melts having low surface energy can favorably wet and permeate into nanochannels due to wetting actions. Thermo-pumping technology<sup>6,7</sup> and electric fields also<sup>8</sup> have been applied to boost the capillary flow of fluids in nanochannels. Particularly, the wetting of porous templates with polymer melts and solvents are a highly effective way to produce polymer nanotubes or nanorods.<sup>9</sup> Anodized aluminum oxide (AAO) or silicon templates with uniform pore diameters and high aspect ratios can be used as templates. The accessible pore diameter range is from 25 to 100 nm from these templates.<sup>10,11</sup>

A crucial factor for the fabrication of nanostructures of polymers is the favorable nanoflow behavior of polymer melts through nanochannels. Comparing with the fluidic

hydrodynamics of simple liquids through micro- or macrochannels, shows that the nanoflow behavior of polymer melts is affected much more by nanoscale effects and surface interactions.<sup>12</sup> Owing to the adversity in achieving an appropriate flow of liquid in nanochannels, many researchers' concentration is about the simulations of nanoflow of simple liquid in nanochannels mainly using molecular dynamics and Monte Carlo methods for the study of tunable size of nanotubes and nanorods<sup>13-16</sup>.

The highly effective way to produce polymer nanotubes or nanorods is the wetting of porous templates with polymer melts and solvents<sup>9,17,18</sup>. It depends upon the used material for nanorods or nanotubes can be obtained. Wetting with melts of low molecular weight organic materials, e.g., liquid crystals, yields in nanorods and with high molecular weight polymers usually in nanotubes.<sup>9</sup> Further structures, besides nanotubes and nanorods, can also be obtained by an additional annealing step after the nanotube production. Russell et al. obtained regular void structures by annealing polymer nanotubes.<sup>9,17</sup>

The unique features of nanostructured materials has led to develop new miniature devices that exhibit unique capabilities which are not available in larger scale devices. In practical applications of nanochannels, nanotubes and nanorods fibers have the ability to fill, transport, and release molecules in a controlled manner.<sup>19</sup> Nanotubes and nanorods or arrays formed by wetting of template with polymer melts are of interest for drug delivery applications, photonic crystals, sensor applications, catalysis, and optoelectronics as demonstrated in a set of papers.<sup>1,12,19-25</sup>

The aim of this short review is to present the main outlines of investigation and to give an updated comprehensive description of the most important aspects related to the fabrication of polymer nanotubes/nanorods by wetting of nanochannels in the nanoporous template of polymer melts. There have been several other reviews related to template fabrication and related subjects that may be of interest to the reader.<sup>26-28</sup> For example, earlier experimentation on the wetting of polymer nanofilms through nanochannels are studied and reviewed in detail by Krausch.<sup>26</sup> We will also not give consideration to segregation and wetting phenomena at interfaces of nanochannels of porous alumina templates because these have been discussed by Budkowski.<sup>27</sup> For an overview and knowledge of relevant and important description, the interested reader is advised to consult the review by the Gennes,<sup>28</sup> which is more recommended.

The review is organized as follows. We first discuss theories about flow behaviors of polymer melts through nano channels in section 2 then in section 3, we will inform readers how to control polymer melt flow parameters. In sections 4, focus on the fabrication of polymer nanomaterials by template wetting. In the last section, the applications of the above polymer nanomaterials will be discussed from different aspects. Finally the conclusion and outlook are also given.

## 2. Theory

Several models for prediction of flow exist through nanochannels or capillary, which may describe the phenomenon according to different perspectives, including the surface effects and shear rate dependent models.<sup>29</sup> Three flow models including capillary Flow Model, Slit flow model and Artificial Neural network (ANN) are appropriate to analyze the rheological behavior and to estimate the molten polymer melt flowing through micro/nanochannels of square cross section.<sup>30,31</sup>

### 2.1. Capillary Flow Model

Firstly, this model is used to examine viscous-dominated capillary wedge channel flows for which analytical solutions are in hand.<sup>32</sup> defined that, insufficient fluid/polymer melt is present to fill all of the pores of nanochannels, so that air fills the remaining space, the medium is known as "unsaturated," or the flow is said to be "capillary flow. This is the simplest type of flow problem deals with "saturated" media in which all of the pores are completely filled with one homogeneous liquid.<sup>33,34</sup>

The most common instrument used for measuring the melt viscosity is capillary viscometer or capillary rheometer depends upon shear rate and temperature, the molten polymer is forced to flow by a piston under a given pressure through a capillary. By the amount of melt exiting, the capillary per unit of time and the required pressure drop across the capillary one can calculate the melt viscosity at a specified shear rate.<sup>30</sup>

The apparent shear rate ( $\dot{\gamma}_{w(app)}$ ) and the apparent shear stress study on rheological behavior of polymer melt ( $\tau_{w(app)}$ ) at the wall for Newtonian fluids is given by

$$\dot{\gamma}_{w(app)} = 4Q / \pi R^3$$

$$\tau_{w(app)} = \Delta P R / 2L$$

In these equations,  $R$  is the radius of the capillary having length  $L$ , and  $Q$  is the volumetric flow rate through the capillary under a pressure drop  $\Delta P$  along the capillary. Furthermore, two corrections are commonly applied to capillary data in order to obtain the correct viscosity of polymeric fluids. The Rabinowitsch correction<sup>35</sup> corrects the rate of shear at the wall for non-Newtonian liquids. That is

$$\dot{\gamma}_{w(real)} = (4Q / \pi R^3)(3/4 + b/4)$$

$$\tau_{w(real)} = (\Delta P - P_0) / (2L/R)$$

Where  $b$  is the slope of  $\log \dot{\gamma}_{w(app)}$  versus  $\log \tau_w$  (correlated in a bi-logarithmic coordinate system) In addition, the Bagley correction takes care of the non-ideality arising from viscous and elastic effects at the entrance to the capillary. The effective length of the capillary is greater than its true length. The  $P_0$  is the pressure drop corresponding to a capillary of zero length for a given rate of shear. After correction, the real viscosity of molten polymer can be obtained by dividing the real shear stress by real shear strain rate as follows.

$$\eta_{real} = \tau_{w(real)} / \dot{\gamma}_{w(real)}$$

For the typical  $\log \eta$  and  $\log \dot{\gamma}$  curve, over the usual accessible shear rate range, the viscosity decreases nearly linearly with the shear rate. This is known as the shear-thinning behavior.

This model helps to determine the impact that shear and elongational flow have on the breakage of aspen fibers in a polypropylene matrix as well as helps to study the velocity distributions, velocity profiles, pressure drops, and vortices at the capillary entrance of rubber compound.<sup>36,37</sup>

Capillary flow behavior is characterized by hysteresis effects which can't be negligible, sometimes amounting to a factor of 30. which makes it limit to use.<sup>29,34</sup>

### 2.2. Slit Flow Model

A statistical mechanical based model which is based on Green-Kubo relations for calculating slip length.<sup>38</sup> This model computes for the slip length as a ratio of a phenomenological parameter and friction factor to the shear viscosity. Furthermore, this model might be used in conjunction with Navier slip boundary condition<sup>39</sup> to obtain the velocity profile during a flow. Friction factor is directly related to the fluctuations of wall fluid interaction force, which can be demonstrated equilibrium molecular dynamics (EMD) simulations. Hydro-dynamic location of the wall can also be computed using EMD correlations. There are some limitations of this model for small pores<sup>40</sup> in which wall-fluid potential owing to confining surfaces overlap.

For the mass production purpose, recently, some specific designed devices have been developed having numerous duplicated microstructure, elements. Nisisako et al.<sup>41</sup> described a planar glass chip with 16–256 microchannels arranged circularly to form monodispersed emulsion. Geerken et al.<sup>42</sup>, utilized the perforated

metal nozzle plates to introduce oil-in-water and water-in-oil emulsion by shear-induced emulsification but these methods or ways didn't remove clearly the Blockage and clogging so one dimension of T junction is enlarged based upon slit model called slit microchannels having low machining complexity and cost. In recent work, using polymethyl methacrylate (PMMA) slit-like microchannel devices with different geometric structure are made which flow pattern maps at crossing flow mode and perpendicular flowmode were carefully figured out under high two phase flow rate.<sup>43</sup>

The instrument for measuring the behavior of the molten polymers through nanochannels is the slit viscometer<sup>30</sup>, which has the same measuring principle as the capillary rheometer. The molten polymer in a reservoir is also forced to flow by a piston under pressure through a slit die. The amount of polymer exiting the slit die per unit of time ( $Q$ ) at a given pressure drop ( $\Delta P$ ) allows one to calculate the viscosity. The apparent shear rate and the real shear stress at the wall for Newtonian fluids after Walter correction provides the rate of shear at the wall for non-Newtonian liquids.<sup>30</sup>

$$\dot{\gamma}_{w(\text{real})} = (6Q / w h^2) (2/3 + b/3)$$

$w$  and  $h$  are the width and thickness of the slit having length  $L$ .  $Q$  is the volumetric flow rate through the slit under a pressure drop  $\Delta P$  along the slit. In addition, two corrections are commonly applied to slit data in order to obtain the correct viscosity of polymeric fluids. Where  $b$  shows slope of  $\log \dot{\gamma}_{w(\text{real})}$  versus  $\log \tau_w$  that is similar to the Rabinowitsch correction in the capillary flow model.<sup>29,30</sup> Furthermore, the edge effect of shear stress shall be carried out when the ratio of the width to thickness is less than 10. The wall shear stress is

$$\tau_{w(\text{real})} = (wh/2(w+h)) (-\Delta P_{(\text{real})} / L)$$

After studying these models it was determined that these models are not suitable in nanochannels of porous alumina during template wetting of polymer melts to predict the exact flow behavior because of hysteresis effect and limitation of models for small pores.<sup>20,29,30,32,34,40</sup> So to resolve this issue (predict the flow behavior through nanochannels of porous alumina) there was a need for a computational method or novel technique, so for this purpose an artificial neural network (ANN) approach was introduced.

### 2.3. Artificial Neural Network (ANN)

It has been perceived that the Young - Laplace equation, capillary flow model and slit flow model is not more appropriate to estimate the wetting process specially through nanochannels<sup>41,42,44,45</sup> In this case, a different methodology, named, ANN is introduced for modeling and anticipating the flow behavior of polymer melts through nanochannels.<sup>18</sup> For example, the imbibition length of the polyethylene melt through nanochannels by nanoporous alumina templates is measured by this method. ANN is used to forecast the relationship between the length of wetting as output parameter and other parameters (time, temperature, diameter and surface properties of inner walls) as input variables, as shown in Fig 1. The designed ANN

was then used to measure the wetting length of the nanochannels for cases, which were not informed by the wetting experiments.<sup>46,47</sup> Recently, interesting experiments were done related to the infiltration of highly viscous liquids in nanopores comparable with or even smaller than end-to-end distance.<sup>46,51</sup>

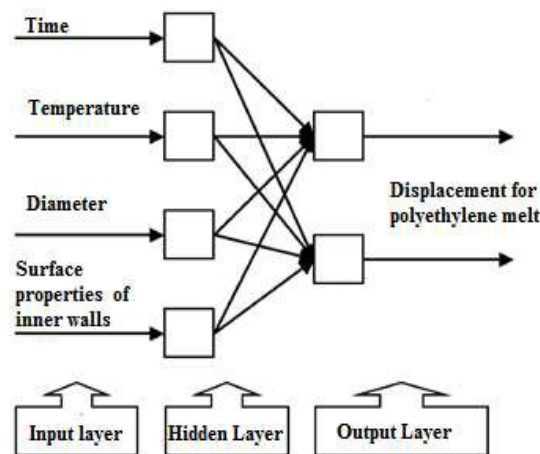


**Fig.1.** Diagram of a typical Artificial Neural Network (ANN). ANN has three layers (i.e., input, hidden, and output layers) including four neurons in the hidden layer and the number of variables is 4 and 2 in the input and output layers, respectively. Reprinted with permission from ref 20. Copyright 2009 Springer.

The ANN Toolbox encapsulated in Matlab 7.0 was used to get the displacement of the polymer melt as a function of time, temperature, diameter of the nanochannels, and surface properties of the inner wall of the nanochannels of nanoporous alumina templates.<sup>52</sup> The input layer of the network consists of time, temperature of the nanochannels, and surface properties of the inner wall of the nanochannels, while the output layer of the network shows the displacement of the polyethylene melt in nanochannels. In this enquiring process, the best architecture of network was obtained which can predict flow behaviour at given conditions of polymer melts through nanochannels<sup>20,46</sup>

Furthermore, an ANN neglects a relatively large amount of noise or variations during dealing with problems, while it derives principle rules regarding a given problem. Interesting, these errors and problems can be observed in simulations, such as molecular dynamics and Monte Carlo simulations, which have been used to simulate flow of simple fluids in nanochannels.<sup>53-57</sup>

### 3. Polymer Melts Flow Dependence

Generally, the main factor for any liquid to flow is viscosity, low viscosity approves that the forces between liquid molecules and surface are weak and vice versa. Basically there is need to control the viscosity to get the better flow of liquids

or polymer melts through nanochannels<sup>58</sup> The main reason to control viscosity is to control wetting rate phenomenon that is verified by Lucas – Washburn equation,<sup>59</sup> which can be used to calculate the nanoflow rate of polymer melts in nanochannels.<sup>52</sup> For the process of inquiring of flow behaviour of polymer melts in through-hole nanochannels, the active or dynamic parameters such as driven force  $p$ , displacement  $l_t$  and rate  $dl_t/dt$  are brought into consideration as illuminated in Fig 2. Owing to the high surface energy of alumina, polymer melts having low surface energy can be wetted the surface in a partial or complete wetting regime and the wetting driven force  $p$  from high-energy surface can be explained by the given following Laplace equation.<sup>46,47,60</sup>

$$p=2\gamma\cos\theta/R$$

Where  $\gamma$  is surface tension of polymer melts on alumina surface,  $\theta$  is contact angle,  $R$  is hydraulic radius and equal to half of the radius of a nanochannel. In particular, the contact angle  $\theta$  is determined by the solid-gas  $\gamma_{SG}$ , solid-liquid  $\gamma_{SL}$ , and liquid-gas  $\gamma_{LG}$  interfacial tensions as shown in Fig 2.

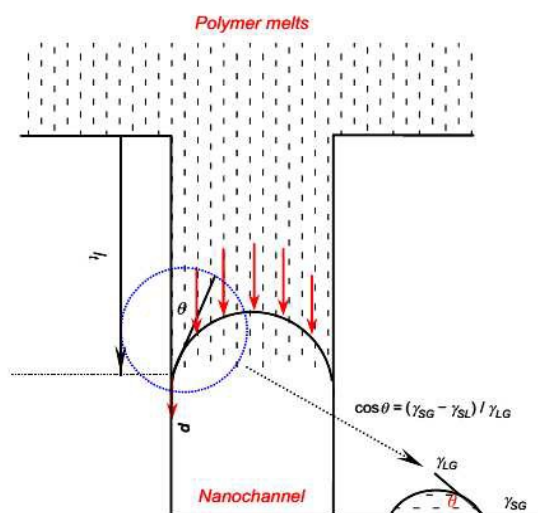


**Fig.2.** Dynamic flow parameters of polymer melts in nanochannels, the  $p$ ,  $l_t$ , and  $\gamma_{SG}$ ,  $\gamma_{SL}$ ,  $\gamma_{LG}$  are driven force, displacement, contact angle and solid-gas, solid-liquid, liquid-gas respectively interfacial tensions, respectively. Reprinted with permission from ref 47. Copyright 2007 Elsevier Ltd..

Polymer melts flow in nanochannels can be affected by different parameters such as temperature, diameter, surface properties and nanochannels sizes.<sup>20,47,60-63</sup> In this short review, it is briefly discussed about the effect of temperature, diameter and surface properties

### 3.1 Wetting Temperature

Understanding the temperature-dependent nanofluidic transport behaviour is critical for developing of

thermomechanical nanodevices.<sup>64</sup> Owing to the relatively less severe confinement effect, both the effective shear stress and nominal viscosity decrease with the increase of temperature. The thermal effect becomes coupled with the nanotube size and transport rate effects, where as in smaller tubes at higher flow rates, the transport resistance is more temperature sensitive, whose energy density can be controlled through temperature.<sup>64-66</sup>

When the temperature of polymer melts is much higher than melting temperature, polymer melts will rapidly wet and flow in nanochannels<sup>47</sup>. On high energy surfaces, the effect of wetting temperature  $T_w$  on nanoflow of polymer melts in nanochannels can be attributed to the wetting transition of melts. For the wetting of solid substrates by liquids, a temperature  $T_w$  is prophesied for a wetting transition from partial to complete regime, where  $T_w$  is known as the wetting transition temperature.<sup>67</sup>

For demonstration, considering an example of polyethylene, influences by the effect of temperature.<sup>20,47</sup> The wetting temperature takes an important part in the displacement of polyethylene melts into nanochannels having a diameter of 80 nm and a length of about 50 mm was used and the wetting time was adjusted as 60 min. The rely of displacements ' $l_t$ ' of polymer melts through nanochannels upon wetting temperature is shown in Fig. 3 and the DSC melting curve of polyethylene is also presented. When the wetting temperature reaches 160°, the polyethylene melts, having low viscosity start wetting the inner walls of nanochannels in a complete wetting regime. Owing to the limitation of maximum length of nanochannels, it should be noticed that the displacement of melt is only determined in the scale less than 50 mm. The higher flow displacement per chance can be accomplished at wetting temperature greater than 160° because of the decrease in viscosity of melts with the increase of temperature.<sup>47</sup>

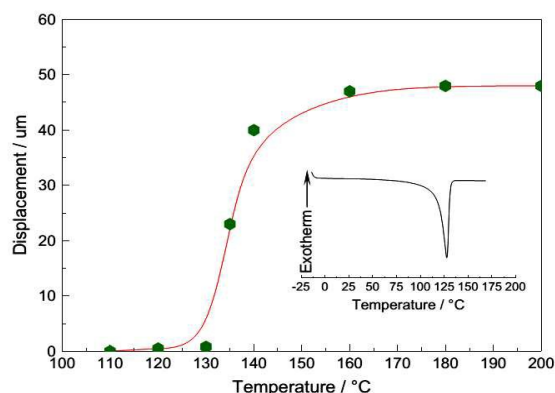


**Fig.3.** The relationship between the displacements of polyethylene melts in nanochannels and the wetting temperature within the same wetting time. Reprinted with permission from ref 47. Copyright 2007 Elsevier Ltd.

### 3.2 Size of Nanochannels

Besides, the system temperature the size of nanochannel can be further optimized by taking into account the pore size of nanochannels affects in transporting polymer melts from nanochannels, a variation of the liquid phase, and surface modification. Since the transport behaviour changes when ions are added to the liquid phase<sup>64,66</sup>. Decreasing the pore diameter may cause the transition from wetting state to non wetting state.<sup>9,61,62</sup> Ordered porous alumina is depicted by high regular alignment of parallel pores having sharp diameter distribution and uniform pore depth, the tiny opening demonstrate high regularity and specific macroscopic orientation over large areas (on the order of square centimeters) which becomes the source to give us nanorods and nanotubes with different diameter sizes of nanochannels.<sup>9,68</sup>

Similar as demonstrate above quotation, considering an example of polyethylene, influences by the size of nanochannel<sup>20,47</sup> at the wetting temperature of 160°C, the results show that the flow rate of polymer melts flow through nanochannels on wetting also depends upon the diameter of nanochannels and the polymer melts having larger size in the range of 80-220 nm are easier to be wetted into the nanochannels. If one observes three types of nanochannels with different diameters, infiltration displacement of melts have a maximum length of nanochannels (50 mm) at 60 min. This shows that the wetting of polyethylene melts into nanochannel is a rapid process. Furthermore, the increment in the flow rate with the increase of the diameter of nanochannels can be seen. It indicates that the polymer melts are easier to be wetted into the nanochannels having larger size in the range of 80-220 nm as shown in Fig 4.<sup>47</sup>

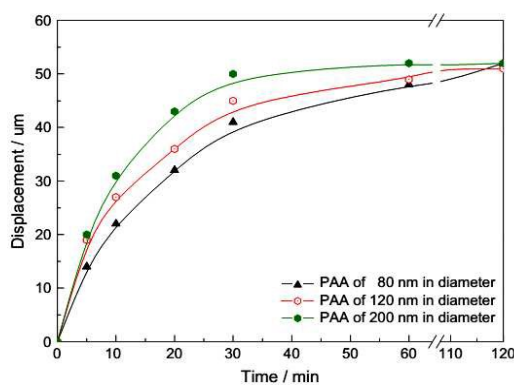


**Fig.4.** The relationship between the displacements of polyethylene melts in nanochannels of different diameters and wetting time at the wetting temperature of 160 °C. Reprinted with permission from ref 47. Copyright 2007 Elsevier Ltd.

### 3.3 Properties of Nanochannels

The nanoflow behavior of polymer melts can be affected by the properties of nanochannels such as roughness of nanochannels.<sup>69-72</sup> The flow behavior of polymer melts under variety of surface conditions have been investigated.<sup>73-75</sup> one of them is by modification of the nanochannel surface by a surfactant (AuNPs) of various sizes, by addition of surfactant the surface energy of the nanochannel is changed. In comparison with Pure AAO, the flow of polymer increases as the uniform distribution of a 5 nm AuNP monolayer on the nanochannel wall enhanced, because of an increase in surface energy. A further increase in the size or distribution of AuNPs in the nanochannel increase the surface roughness of nanochannels, and the flow behavior of the polymer melt was significantly affected in nanochannels.<sup>66,76</sup>

To adjust the wettability property, the alkylsilane self-assembled monolayers (SAMs) having significantly low surface energy was often used on alumina surface. The self-assembled monolayers on inner walls of nanochannels in PAA template are formed after the hydrolysis, condensation and curing at high temperature of octadecyltrimethoxysilane.<sup>47,70, 77-79</sup>

Comparing SAMs treated nanochannels and native alumina nanochannels at the same wetting temperature, we come to know that the infiltration displacements and rate of polymer melts into SAMs entreated nanochannels are less and lower than those in the native alumina nanochannels, it can be seen in Fig 5. This is because of the decrease in surface free energy on alumina surface entreated by SAMs that is low surface free energy material. This phenomenon can also be seen for the contact angle and surface free energy of n-hexadecane (non-polar, low molecular weight analogues of polyethylene) on the octadecyltrimethoxysilane modified alumina surface or silicon wafer.<sup>69,80</sup> By considering contact angle, the static contact angle of n-hexadecane on the native alumina surface (3°) is less than the SAMs treated alumina surface (4°) shown in Fig. 5 it uncovers that the solid-liquid interaction and high surface free energy between surface and melts lead to significant flow of polymer melts in nanochannels at the wetting stage.

### 4. Nanofabrication of Polymers

The process of making functional structures with arbitrary patterns having minimum dimensions currently defined  $\leq 100\text{nm}$  is known as nanofabrication.<sup>81</sup> There are many nano/microfabrication techniques used for fabrication of polymer nanotubes or nanorods.

Electron beam lithography has been used to create surface topographies at the nanometer scale for studying cellular growth and behavior on these surfaces<sup>82, 83</sup>. This technique involves the use of high-energy electrons to expose an electron-sensitive resist. Both positive and negative type resists are available. Unlike photolithography, a physical mask is not needed to pattern the surface with the beam of electrons. The resolution of this technique takes many factors into consideration, including electron scattering

in the resist and backscattering from the substrate. With optimization of the process, Electron beam lithography has ability to produce single surface features about 3–5 nm.<sup>81, 83</sup> Fabrication using Electron beam lithography can be possibly time consuming and costly because of change in resolution with time.

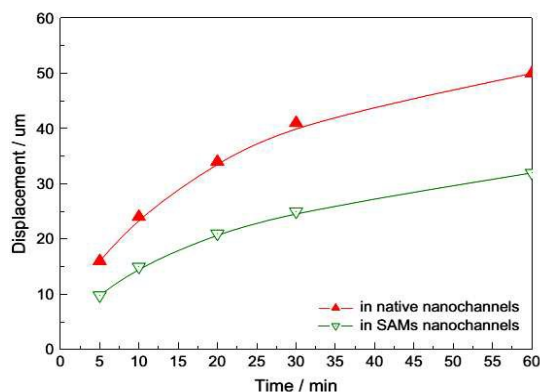


**Fig.5.** The relationship between displacements of polyethylene melts in nanochannels with different inner walls surface properties at the wetting temperature of 160°. Reprinted with permission from ref 47. Copyright 2007 Elsevier Ltd..

A unique method for creating nanoscale topographical features for use as cell substrates is through the use of polymer demixing. Polymer demixing involves the spontaneous phase separation of polymer blends. This process is a quick and inexpensive method for creating cell culture surfaces with nanoscale feature that can be used to create topographies similar to those commonly used to study cell growth on nanostructured surfaces.<sup>81, 85-87</sup> Polymer demixing does not lend it for creating ordered arrays of structures or structures with precise geometries. The features created using polymer demixing are somewhat uncontrollable in the horizontal direction, yet very precise control can be achieved in the vertical direction. Polymer demixing may not be ideal for creating model surfaces to study cellular interactions with nanoscale features.<sup>81, 88-90</sup>

Another inexpensive method for creating nanoscale topographies is colloidal lithography. This technique allows for the production of surfaces with controlled heights and diameters. Colloidal lithography involves the use of nanocolloids as an etching mask. These nanocolloids are dispersed as a monolayer and are electrostatically self assembled over a surface. Only the biologically relevant patterns such as nanocolumns and nanopits can be created well with this method<sup>91, 92</sup>

The means of producing nanoscale features on the surface of a material by soaking is chemical etching. Generally, etchants are hydrofluoric acid (HF) and sodium hydroxide (NaOH). Nanometer-scale roughness on every surface of the scaffold can be created by chemical etching using NaOH. Roughness features smaller than 100 nm were created in this way. This process is essentially a surface treatment and may not produce structures with any prescribed geometry or organization. Roughness features smaller than 100 nm were created in this way.<sup>81, 93</sup> Three dimensional scaffolds are

getting interest in tissue engineering for this purpose phase separation a technique for which no special equipment is required and allows for three-dimensional scaffolds in the sub-micron range can be created with fibers. This process consists of five steps Polymer dissolution, phase separation and gelatin, solvent extraction from the gel, freezing followed by freeze drying in water<sup>94</sup>. This process sometimes needs expensive solvent which makes it limit to use.<sup>81</sup>

A unique technique, self-assembled nanofibrous scaffolds involve the use of polymers that undergo self-assembly to form scaffolds consist of a matrix of nanofibers. Molecular self assembly is an alternative to lithographic. The key to the self-assembly of these scaffolds is the engineering of the molecules themselves. This is a common technique for creating these self-assembling scaffolds. But its time consuming, Time for adsorption of polyions onto surface ranges from minutes to hours.<sup>95,96</sup>

Summarizing it, explains that because of limitation of other technique such as severe conditions, tedious fabrication, special equipment, and expensive reagents,<sup>97</sup> a suitable technique is introduced that is template wetting as demonstrated in following section.

#### 4.1. Fabrication of Polymer nanotubes/nanorods by Template Wetting

A template-directed approach for preparing polymer nanomaterials has been led by Martin and his co-workers since the early 1990s,<sup>98</sup> in which the synthesis of uniform-sized nanomaterials is formed by using membrane templates with the monodisperse cylindrical pores in terms of the diameter and length.<sup>19, 99</sup> The wetting of porous AAO templates with polymer melts and solutions or polymer-containing mixtures is a simple and versatile method for the formation of tubular structures having diameters ranging from a few micrometers to nanometers. The tube walls can be formed of a number of materials, some of them have thus far been impossible to use altogether or very limited in their aptitude to be included into nanostuctures. It is possible to modify nanotubes in many varieties by using template wetting, through the controlled generation of pores or the embedding of nanoparticles into the walls.<sup>100</sup>

Since Steinhart et al.<sup>101</sup> pioneered the preparation of sundry polymer nanostructures by wetting polymer melts into nanopores of AAO templates, the process of template wetting proved as a one fold and efficient method even in industrially inspiring fabrication method.<sup>101-108</sup> basically, it consists of two steps, one is fabrication of template and second is infiltration of polymers onto nanopores as shown in scheme 1. In this way, the first part is about AAO templates, and a second part covers the infiltration process of polymers into nanopores.<sup>109</sup> Mainly wetting is primarily controlled by the molecular weight while keeping the quality of the solvent and the solution concentration constant in template wetting.<sup>100</sup> In general, three

main types of nanostructures formed by template wetting that are solid nanorods, nanotubes, and cylindrical nanostructures with a periodic arrangement of voids along the axis. To verify the correlation between the molecular weight and formation of structure, the structures formed via template wetting is displayed in Table 1.<sup>9</sup>

**Table 1:** Types of cylindrical nanostructure available from Template wetting for various molecular weight of PS. Adapted from ref 9 with permission. Copyright 2008 American Chemical Society.

Mol wt(g/mol)	Nanorods	Regular void structure	Nanotubes
1890	√		
4850	√		
7000	√		
17300		√	
35600		√	
75000		√	
96000		√	
133000			√
184000			√
248000			√
319000			√
601800			√

Where “√” represents the transformation of the polymer structure with respect to molecular weight.

In the range up to 7000 g/mol solid nanorods are significantly viewed for molecular weights, in the range about 17,000 g/mol up to about 75,000 g/mol regular void structures are dominant, and at the end nanotubes are common above this range of molecular weights. It must be in consideration that, these three types of structures are not strictly bounded to the molecular weights as mentioned in Table 1. Each of them may also be noticed outside the mentioned ranges but the probability is low.<sup>9</sup>

## 4.2. Fabrication of Polymer Nanotubes by Template Wetting

The polymers having high viscosity, along with melting and glass transition temperature above room temperature, attracted concentration of researcher's to notice straightly the

behavior in nanotubes and nanochannels.<sup>110</sup> To overcome imperfections, the actual observation of the solidified, cross-linked or cooled-down drop has been used to introduce knowledge about the wetting process.<sup>111</sup> So for this purpose thermal treatment of PVDF-coated CNTs, SEM observations showed both clamshell and barrel like droplets on the outer side of carbon nanotubes. The estimated contact angle of pure PVDF drops had more than 60°, but the addition of maleic acid anhydride (MAH), in ppm quantities causes to lower the contact angle about to ~20°, essentially improvement in the adhesion of the polymer to the CNT, fundamentally necessary for operative load transfer from the matrix to the fiber in polymer-CNT composite materials. The objective to encapsulate polymer melts inside carbon nanotubes is, to use the polymer as a cap for the liquids having lower molecular weight (chiefly water) already inside the CNT.<sup>112</sup> Within nanotubes and microchannels, this has been testified for surfactants, nanoparticles in solution and low molecular weight fluids. Actually, this process based on wet reversible insertion of molecules of polycaprolactone (PCL) inside carbon nanotubes filled with an insoluble liquid. In one experiment, the CNTs were occupied by water and dunked in a solution of PCL in toluene. The PCL molecules are guided by self-sustained diffusion to the CNT open ends, but PCL cannot easily move into CNT cavities that are taken up with water, that is immiscible with toluene and a non-solvent for PCL. As a moment, when the molecules of PCL confront water in CNTs, they pile up and sometimes cap the tube entrances.<sup>110,111,113</sup> By observing above quotation it is observed that Hyperbranched polymers are popular because of fabrication by temple wetting<sup>110</sup>

The patterning of hyperbranched polymer (HBP) films on the substrates is receiving more and more attention. HBPs have advantages over linear polymer by the template wetting process.<sup>113-115</sup> HBPs can be widened to motley polymeric matrices to actualize nanopatterns, and can be beneficial for modified artificial superhydrophobic surfaces as well. It should be indicated that the nanoparticles by template wetting are not restricted to only HBPs, other HBPs may be suitable to be taken into account as processing aids. However, the ability between the polymer matrix and dispersed phase as an important factor should be fully taken into account. In this short review, we are discussing just an example, there are many other hyperbranched polymers are participating in the formation of nanotubes.<sup>12,112,113</sup>

Particularly, the effect of β-cyclodextrin-based hyperbranched polymers for the formation of micro/nanopatterns by template wetting is studied well.<sup>12</sup> Polystyrene (PS) is employed as the polymeric matrix and β-CD or HBP (β-CD) as the dispersed phase. The micro/nanopatterns were formed via melt wetting of AAO template with a nanochannel diameter about 200 nm and a length of about 60 μm. The wetting temperature and time for these PS-based melts in AAO templates were adjusted as 170

$^{\circ}\text{C}$  and 15 min, respectively. In the procedure of AAO template wetting tepee-like bundles as micro/nanopatterns, consists of irregular polygon “podium” and “valley” structures, can be shaped. The degree and place of micro/nanopatterns can be distinctly enlarged with the increment in  $\beta$ -CD content or  $M_w$  of HBP ( $\beta$ -CD). The outcome structure of micro/nanopatterns after instigate  $\beta$ -CD or HBP ( $\beta$ -CD) including PS melts in AAO templates as shown in Fig. 6.<sup>68</sup> It can be seen from Fig. 6A, the pure PS nanofibers/nanotubes have the capability to form aligned arrays in the wetting process. This may be ascribed to the formation of one dimensional nanostructure having aspect ratios (about 1/25).<sup>54-56</sup> By adding  $\beta$ -CD or HBP ( $\beta$ -CD), content 5% of  $\beta$ -CD having aspect ratio is about 1/130, (Fig 6B) and HBP ( $\beta$ -CD) with  $M_w$  of 83, 290 g/mol having aspect ratio is about 1/80, (Fig. 6C) in the PS matrix, results in short, aligned nanofibers/nanotubes in case of low aspect ratio, longer ones with high aspect ratios are formed. In addition, the enhancement in nanoflow rate is more noticeable as the  $\beta$ -CD content or  $M_w$  of HBP ( $\beta$ -CD) is increased, which directly cause of resulting in the formation of longer nanofibers/nanotubes during the wetting process (Fig. 6D and E).<sup>12,60</sup>

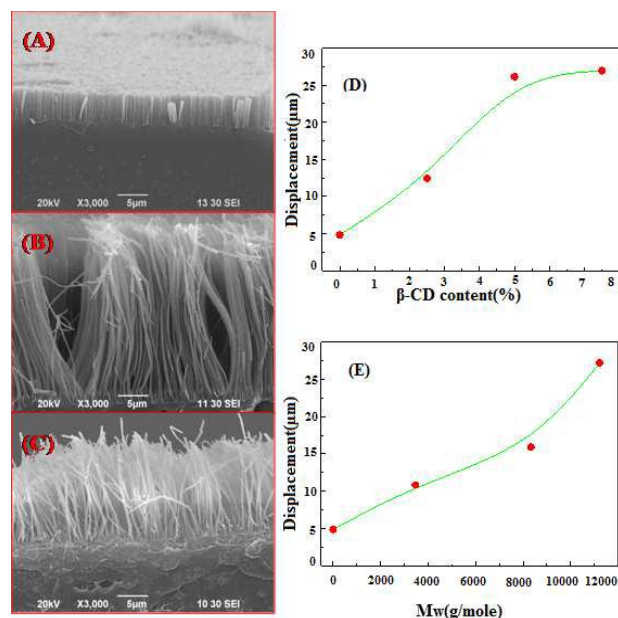


**Fig.6.** Typical SEM cross-section images of nanorods/nanotube arrays formed at the wetting time of 15 min and the wetting temperature of  $170^{\circ}\text{C}$ : (A) the pure PS, 25 (B) PS/ $\beta$ -CD(95/5), (C) PS/HBP( $\beta$ -CD) [95/5, the  $M_w$  of HBP( $\beta$ -CD) is 83 290 g/mol]. The dependence of displacements of PS/ $\beta$ -CD in AAO templates on  $\beta$ -CD content (D) and of PS/HBP ( $\beta$ -CD) in AAO templates on the  $M_w$  of HBP ( $\beta$ -CD) (E).<sup>60</sup> Reproduced by permission of The Royal Society of Chemistry

For the preparation of nanotubes to be suitable for templates, pore walls of porous membranes must have high surface energy.<sup>60,99,107,108</sup> Precursor film is formed, as a droplet of a low-energy liquid contacts with a high-surface energy.<sup>116</sup>

Most of polymer melts and solutions are deliberated as low-energy materials Whereas inorganic materials are deliberated as low-energy materials.<sup>117</sup> So, polymer melt or solution will spread instantly to a thin film by placing it on a substrate having high energy surface,<sup>60</sup> and thickness of films starts from a few angstroms to nanometre range during the spreading proceeds. In case of polymer melt or solution during contacting with the surface of a porous template, resulting in wetting phenomenon. Similarly, a thin film is formed and spread on the inner surface of the pores consequence in polymeric nanotubes, interestingly; wall thickness increases as time increases, and finally may end in nanorods and nanowires. Besides the wetting properties of the pore walls a lot of other factors also affect the pore filling that are the inevitable increment of a solid layer on the pore walls, capillary flow of the solution into the pore, and phase separation of the polymer.<sup>118</sup> Wetting of porous templates with polymer melts is same as wetting of porous templates with a solution.

As PS having molecular weights about 75,000 g/mol seen to give us rise in the formation of a thin wetting layer. From that way we can get nanorods easily from templates. In Fig.7 two examples of such types of nanotubes of PS with different molecular weights are shown. Wetting happens to all pore diameters available from the templates in the range of PS molecular weights. Pores diameters limit from 150 to 560 nm go up polymer nanotubes with corresponding outer diameters (Fig 8a).<sup>9</sup>

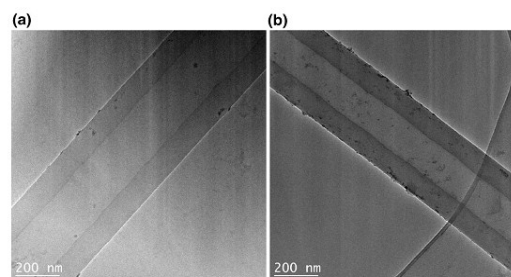


**Fig.7.** TEM images of nanotubes obtained via wetting from solution containing high molecular weight fractions of polystyrene: (a) 96,000 g/mol; (b) 133000 g/mol. Reprinted with permission from ref 9. Copyright 2008 American Chemical Society.

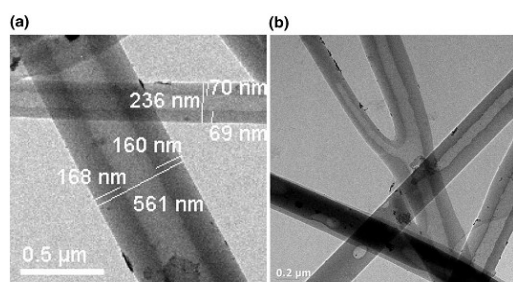


**Fig.8.** (a) Nanotubes with different diameters and wall thicknesses. (b) Branched nanotubes originating from branched pores within the template; the wall thickness changes as a function of the radius of the tubular structures. Reprinted with permission from ref 9. Copyright 2008 American Chemical Society.

In all cases nanotubes with the same wall thickness are composed, which are independent of the molecular weight of the PS used in the wetting. It is fact that the wall thickness depends upon the pore radius. It is also an interesting observation that same wetting also happens at branches within the range of the pore structure. These branches show up as branched nanotubes as shown in Fig 9b. Similar as the radius of branches varies, the thickness of the walls entirely varies along the branches in. It has already been mentioned as the variation in pore radius become the cause the thickness of the solidified wetting layer within the pores and thus of the resulting nanotubes. Furthermore possible same happens to a variation of the molecular weight of PS.<sup>111, 119-122</sup>

### 4.3. Fabrication of Polymer Nanorods by template Wetting

The molecular weight fractions of PS below 7,000 g/mol move towards complete filling of the pores during the wetting of the templates and thus, after the descent of the solid PS, polymer nanorods were obtained. For this purpose the formation of the nanorods is noticed for oligomeric systems.<sup>113</sup> as shown in Ref. 9, it is observed that nanorods formation is independent of the pore diameter for all molecular weights, but the rod diameter can be directly controlled by the pore radius.<sup>61,62,122-124</sup> These rods do not seem to be completely solid, in fact small irregular holes are distributed on the upper surface of the rods, and sizes of nanorods do not seem to bear any similarity with the rod diameter. Wetting from polymer melts qualitatively same with wetting from the solution, whereas complete pervading of the pores and nanorods formation has been observed for low molecular weight systems confined oligomersystems.<sup>118,123</sup>

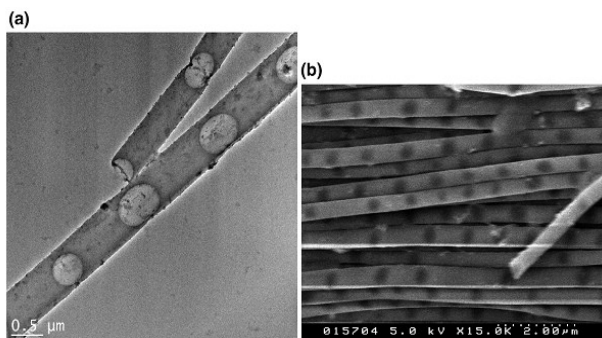


**Fig.9.** Polymer nanostructures resulting from solution wetting for molecular weight fractions with intermediate molecular weights of 35,600 g/mol: (a) TEM image, (b) SEM image.

Reprinted with permission from ref 9. Copyright 2008 American Chemical Society.

In Fig.9, it has been shown some structure after wetting and subsequent extraction. It is clearly seen that regularly spaced void structure along the length of the nanorods are formed. In general, it is interesting that voids are located only within the cylindrical objects and fully covered with the polymer in such a way that the outer wall is completely given by polystyrene. There is an exceptional case in which the voids extend to the surface of the cylindrical objects of PS.<sup>123</sup>

The wetting technique can be easily elongated to form functionalized nanotubes, for example, palladium/polymer composite nanotubes, which wetted the porous templates with a melt containing poly-L-lactide (PLLA) and palladium (II) acetate under atmospheric conditions. Wetted PLLA/palladium (II) acetate film covered the pore walls. Afterwards the template can be strengthened in vacuum at temperatures of up to 300°C to degrade PLLA<sup>123</sup> and to reduce Pd. In next wetting step, molten PS was introduced, so that Pd/PS composite tubes were obtained. As briefly explained in this short review, template wetting has a prominent potential in providing different size of nanotubes for a wide range of applications in nanoscience.<sup>62</sup>

## 5. Application

In general, it is well clarified that ordered polymer nanostructures may have many new and unique potential applications a lot of distinct technological areas including tissue engineering and drug delivery systems, data storage, magnetic sensors, etc.<sup>125-131</sup> In this section, we will review some of proposed applicable materials namely one-dimensional nanostructured polymer fabricated by template wetting. Template synthesis has proven to be a broad method to yield tubes of different materials and sizes.<sup>124</sup> The ability to change the size of the nanotubes or nanorods according to the application at handcrafts nanotubes attractive for biological applications, such as drug delivery, DNA detection and gene transfection. Furthermore, the structure or shape of the nanotube allows for high cargo capacity. Because of the different function of the inner and outer surfaces of nanotubes, there are infinite possibilities for nanotubes in biomedical Nanotechnology as well as in bioseparation and biosensors.<sup>132</sup>

### 5.1 Nanotubes for Drugs and Gene Delivery

Mostly the use of nanotubes is in drug release systems, because of their void application in medical field, similarly nanostructured materials for tissue engineering as well as nanofibers for wound healing while bone tissue engineering is an important aspect. In the following paragraph, some examples for the application of nanostructured materials in medicine are presented.<sup>133</sup> It is still under research about the best delivery vehicle for payloads, such as drugs, DNA, enzymes or other bio

molecules, has still to be developed. Delivery systems are composed to assuage such problems as failure to reach the targeted site, toxic therapeutic concentrations, and poor solubility. Fabricated heterostructured, magnetic polypeptide nanotubes having submicrometer dimension is synthesized used for drug delivery (Fig.10). The wall thickness, inner diameter, length and outer diameter of prepared nanotubes can be changed by changing the assembly of layers and templates respectively. These nanotubes showed super paramagnetic properties at room temperature, and were employed for DNA delivery. Under magnetic force, these magnetic polypeptide nanotubes can be used as a DNA carrier (Fig10b) Because these tubes have characteristics that can be easily manipulated and changed to specific locations by using magnetic forces, one of its uses is as separators as well as carriers of drugs and agents to targeted sites in vivo as well as in vitro and nanotubes (heterostructured, magnetic polypeptide with submicrometer dimensions).<sup>133,134</sup>

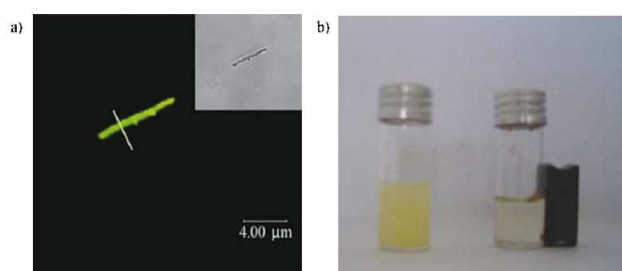


**Fig.10.** CLSM image of plasmid DNA-conjugated magnetic nanotubes and corresponding fluorescence intensity profile. The inset shows the corresponding transmission mode; b) Photograph showing the controlled delivery of DNA-conjugated nanotubes under an external magnetic field. Reproduced from Ref. 134 with permission from The Royal Society of Chemistry.

Silica nanotubes fabricated by template wetting are the most ideal participant because they have, the more advantages as well as a brittle shell, which make us convenient to control the release of the loaded species, such as, using the external stimulus such as ultrasound irradiation. The templated sol-gel silica nanotubes have been deeply studied by Martin and others.<sup>61,62</sup> it is also has been explained that the outer and/or inner surfaces of silica nanotubes can be functionalized to be hydrophobic and/or hydrophilic characteristics with dansylamide and octadecylsilanes.<sup>12,15,117</sup> Hillebrenner and co-workers explained that, by chemical self-assembly, functionalization of the inside pores of silica nanotubes with aminosilane, aldehyde-functionalized PS colloids can be selectively corked to the individual silica nanotubes.<sup>136</sup> Chen et al.<sup>137,138</sup> discussed that template-synthesized sol-gel silica nanotubes can convey or deliver plasmid DNA into monkey kidney COS-7 cells.

## 5.2 Application in Sensors

Conductive polymers have more potential for plastic electronics and sensor applications in a wide range.<sup>138,139</sup> For practical applications, there must be considered that output or signals generated by single nanowire or nanorod based devices is small, signal to noise ratio is small, and finally highly sensitive instruments are required to adjust such devices.<sup>140</sup> If one of the polar crystal modifications can be induced nanotubes were generated from polyvinylidene fluoride, exhibit piezo-, pyro-, and ferro-electric Properties. Template wetting in fact, synthesizes accurate nanotubes from polyvinylidene fluoride.<sup>138</sup> A further more is, within the tubes, the orientation of the axis of the unit cell (a-modification: a, 4.96 Å<sup>o</sup>; b, 9.64 Å<sup>o</sup>; c, 4.62 Å<sup>o</sup>) are well defined. The a-axis is oriented tangentially, along the length of the tubes are b-axis, and the c-axis points radially. The crystal orientation is controlled by curvature. One of the disadvantages is that only the non-polar crystal form is showing off. The researchers focused are still about modifying crystal growth conditions in order to obtain a polar crystal starting from precursor systems; it is an option to get lead zirconate titanate nanotubes actually displaying piezoelectric properties and exhibits ferroelectric switching hysteresis. This approach can be further used to get different kinds of nanotubes of interest in the field of sensors and actuators.<sup>141</sup>

## 5.3 Application in Phonitics

The properties such as nanotubes having diameters corresponds roughly to the wavelength of the light are known to display of photonic crystals. Photonic crystals are characterized by energy ranges that are wavelength ranges, from which light can easily propagate and the material having energy ranges, for which light cannot propagate. The uniform arrangements of nanotubes approachable by the wetting methods may serve as a photonic crystal. If semiconductor quantum structures, such as quantum dots are incorporated in such structures then, still more absorbing effects result according to recent theoretical considerations.<sup>138</sup> In initial study, PS nanotubes containing HgSe and HgTe quantum dots emitting light very effectively have been produced via the template wetting method.<sup>142,143</sup>

## 5.4 Application in Optical Fibers

There is a much faster signal processing in organic material because they easily change their hybridization and much greater state change rate. However, there are problems during producing polymeric materials in a robust optoelectronic fashion such as intensity, sensitivity, long term and low thermal electrical, conductivity instabilities within the polymer due to photochemical effects that are necessary for transport. To fabricate optical waveguides upon chips, polyimide polymers have been used. In 2004, Zhao et al.<sup>142,143</sup> explained a patent in which SWNT-polymer composites consisting 0.1 wt% CNTs and polyimide are discussed for high-

sensitivity and ultra-fast all-optical switch made from. All-optical systems restrict themselves from repeated conversions between electrical and optical signals and they are faster. Woo et al.<sup>144</sup> exposed that the organic light emitting diode, fabricated from poly (m-phenylene vinylene-co-2, 5-dioctoxy-p-phenylene vinylene), PmPV and SWNT (~0.1 wt %), increased oscillator strength in green radiation by about 700% as compared to PmPV alone. From this they analyzed that SWNTs in the composite were answerable for blocking hole transport by forming hole traps in the polymer matrix. This non-linear optical effect could be exhibited to safe optical sensors from high intensity laser beams and in developing new light sensitive shields for helmets.

## 6. Conclusion and Future Outlook

In this article, we reviewed the fundamental theory, fabrication, and application of polymer melts through nanochannels. Although great achievements have been accomplished in this field during the past years,<sup>27,28</sup> there are still many challenges. Wetting studies in nanochannels by polymers melts represent a research area that continues interest for both fundamental science and application. One of them is the theoretical framework for wetting inside nanochannels structure linking with parameters affecting wetting (diameter, temperature and surface properties of the inner wall of nanochannels) and wetting properties (contact angle, surface structure, roughness etc). To complete the theoretical aspect of wetting, we should not forget about the Artificial Neural Network for predicting flow behavior through nanochannels.<sup>4-10,20,46,47</sup> The second area for future research direction is about superhydrophobic surfaces, this area has a clear way in theoretical aspects, but focus is on the stability of superhydrophobic properties and adhesion properties on solid surfaces for long time because of having commercial level application but need to be control production cost. Template wetting is simple and low cost technique to fabricate nanotubes and nanorods because simple fabrication methods and low cost materials are very important for large-scale production and practical applications which need to more research.<sup>111,145,146</sup>

Recently, conductive polymers synthesized by template wetting have great potential for plastic electronics and sensor applications.<sup>147,148</sup> High density polyethylene (HDPE) nanowires array having high thermal conductivity can be used in electronic devices such as computer chips, for containing high temperature. Template-wetting process is used to fabricate Pt electrode nanotubes for the further application in 3D nanotube capacitor because of its stability and low leakage. Similarly If the functional polymers, such as, the poly3-hexylthiophene (P3HT)<sup>11</sup> and [6, 6]-phenyl C61-butyric acid methylester (PCBM) blend having functional micro/nano structures with functionality charge carrier collection will be achieved then it will be potential extensively used in organic solar cells and capacitors.<sup>19,134,148-151</sup>

## Acknowledgment

This work was supported by the National Science Foundations of China (No. 21374088). W.T. thanks the grant from the Program for New Century Excellent Talents of Ministry of Education (NCET-13-0476), the Program of Youth Science and Technology Nova of Shaanxi Province of China (2013KJXX-21), and the Program of New Staff and Research Area Project of NPU (13GH014602).

## Notes and references

MOE Key Laboratory of Space Applied Physics and Chemistry, Shaanxi Key Laboratory of Macromolecular Science and Technology, School of Science, Northwestern Polytechnical University, Xi'an, 710072, P. R. China.

E-mail: happytw\_3000@nwpu.edu.cn

- G. D. Fu, G. L. Li, K. G. Neoh, and E.T. Kang, *Prog. Polym. Sci.* 2011, **36**, 127-167.
- Y. C. Xie, Y. Xu and K. L. Yung, *Polym. Eng. Sci.* 2012, **52**, 205-210.
- G. J. Vancso and G. Reiter, *Adv. Polym. Sci.*, 2006, **200**, 1-37.
- H. Xu, D. Shirvanyants, K. Beers, K. Matyjaszewski, M. Rubinstein, and S.S. Sheiko, *Phys. Rev. Lett.*, 2004, **3**, 206103.
- S. Saritha, P. Neogi and J. C. Wang, *Polym.* 2006, **47**, 6263-6266.
- M. J. Longhurst and N. Quirke, *Nano. Lett.* 2007, **7**, 3324-3328.
- M. J. Park, K. H. Downing, A. Jackson, E. D. Gomez, A. M. Minor, Dcookson, A.Z.Weber and N.P. Balsara *Nano. Lett.* 2007, **7**, 3547-3552.
- I. Vlassiuk, S. Smirnov and Z. Siwy, *Nano. Lett.* 2008, **8**, 1978-1985.
- S. Schlitt, A. Greiner and J. H. Wendorff, *Macromolecules*, 2008, **41**, 3228-3234.
- M. Steinhart, R. B. Wehrspohn, U. Gosele and J. H. Wendorff, *Angew. Chem. Intern. Ed.* 2004, **43**, 1334-1344.
- Y. Luo, I. Szafraniak, N. D. Zakharov, V. Nagarjan, M. Steinhart, R. B. Wehrspoh, J. H. Wendorff, R. Ramesh and M. Alexe, *Appl. Phys. Lett.* 2003, **83**, 440-442.
- W. Tian, K. L.Yung, Y. Xu, L. Huang, J. Kong and Y. C. Xie, *Nanoscale*, 2011, **3**, 4094-4100.
- T. M. Galea and P. Attard, *Langmuir*, 2004, **20**, 3477-3482.
- E. Bonaccorso, H. J. Butt and V.S. J. Craig, *Phys. Rev. Lett.* 2003, **90**, 144501.
- A. Jabbarzadeh, J.D. Atkinson, and R.I. Tanner, *Phys. Rev.* 2000, **E61**, 690-699.
- M. Sbragaglia, R. Benzi, L. Biferale, S. Succi and F. Toschi, *Phys. Rev. Lett.* 2006, **97**, 204503.
- J. T. Chen, M. Zhang, T. P. Russell, *Nano Lett.* 2007, **7**, 183-187.
- J. T. Chen, K. Shin, J. M. Leiston-Belanger, M. Zhang, T. P. Russell, *Adv. Funct. Mater.* 2006, **16**, 1476-1480.
- C. Bae, H. Yoo, S. Kim, K. Lee, J. Kim, M. Sung, and H. Shin, *Chem. Mater.* 2008, **20**, 756-767.
- S. Ahadian, H. Mizuseki, and Y. Kawazoe, *Microfluid. Nanofluid.* 2010, **9**, 319-328.
- S.B. Lee, C.R. Martin, *J. Am. Chem Soc.* 2002, **124**, 11850-11851.
- S. Stefanie A. Greiner, and H. Joachim, *Macromolecules*, 2008, **41**, 3228-3234.
- L.A. Baker, Y. Choi, C.R. Martin "Current Nanosci. 2006, **2**, 243-255.
- M. Wirtz, C.R. Martin, *Sensors Update*, 2002, **11**, 35-64.

25. R. Dersch, M. Steinhart, U. Boudriot, A. Greiner and J. H. Wendorff, *Polym. Adv. Technol.* 2005, **16**, 276–282.
26. G. Krausch, *Mater. Sci. Engg.*, 1995, **14**, 1–94.
27. A. Budkowski, *Adv. Polym. Sci.*, 1999, **148**, 1–111.
28. P.G. De Gennes, *Rev. Mod. Phys.*, 1985, **57**, 827–863.
29. R. Bhaduria and N. R. Aluru, *J. Chem. Phys.*, 2013, **139**, 074109.
30. R.D Chien, W.R Jong and S.C Chen *J. Micromech. Microeng.*, 2005 **15**, 1389–1396.
31. H. H. Saab and R. B Bird, *J. Chem. Phys.* 1982, **77**, 4758–4766.
32. M. M. Weislogel and S. Lichter, *J. Fluid Mech.* 1998, **373**, 349–378.
33. S.V. Mourik, A.E.P. Veldman and M.E. Dreye, *Microgravity Sci. techno.*, 2005, **XVII-33**, 87–93.
34. M.N. Hamblin, A.R. Hawkins, D. Murray, D. Maynes, M. L. Lee, A.T. Woolley, and H.D. Tolley, *Biomicrofluidics*, 2011, **5**, 021103-1 – 021103-6.
35. R.D Chien, W.R. Jong and S.C Chen, *J. Micromech. Microeng.* 2005, **15**, 1389–1396.
36. Y. Wang, S. Shimada, Y. Yamamoto and N. Miyaura, *Mater. Res. Bull.*, 2008, **43**, 251–256.
37. C. Quijano-Solis and N. Yan, *J. Rainforce plast and Composite*, 2014, **33**, 1463–1473.
38. L. Bocquet and J.L. Barrat, *Phys. Rev. E*, 1994, **49**, 3079–3092.
39. L. Bocquet and J.L. Barrat, *Soft. Matter*, 2007 **3**, 685–693.
40. J. Petracic and P. Harrowell, *J. Chem. Phys.*, 2007, **127**, 174706
41. T. Nisisako, T. Torii, *Lab on a Chip*, 2008, **8**, 287–293.
42. M.J. Geerken, M.N.W. Groenendijk, R.G.H. Lammertink, M. Wessling, *J. Membr. Sci.* 2008, **310**, 374–383.
43. G. Liu, K. Y. Wang, Lu, G. Luo, *Chem Engg J*, 2014, **258**, 34–42.
44. R. Helmy, Y. Kazakevich, C. Ni, A.Y. Fadeev, *J. Am. Chem. Soc.* 2005, **127**, 12446–12447.
45. K. Jayaraman, K. Okamoto, S. J. Son, C. Luckett, A. H. Gopalani, S. B. Lee, *J. Am. Chem. Soc.* 2005, **127**, 17385–17392.
46. W. Tian, L. Huang, D. Wang, V.A.L., *Roy. Sci. China Tech. Sci.* 2014, in press.
47. K. L. Yung, J. Kong, Y. Xu, *Polymer*, 2007, **48**, 7645–7652.
48. W. Lu, V.K. Punyamurtula, A. Han, T. Kim and Y.A. Qiao, *J. Materi. Res.*, 2009, **24**, 3308–3312.
49. A. Han, V.K. Punyamurtula and Y. Qiao, *J. Mater. Res.*, 2008, **23**, 1902–1906.
50. A. Han, W. Lu, V.K. Punyamurtula, X. Chen, F.B. Surani and Y. Qiao T. Kim, *J. Appl. Phys.*, 2008, **104**, 124908.
51. X. Chen, G. Cao, A. Han, V.K. Punyamurtula, L. Liu, P.J. Culligan, and Y. Qiao, *Nano. Lett.*, 2008, **8**, 2988–2992.
52. C. Gao and D. Yan, *Prog. Polym. Sci.* 2004, **29**, 183–275.
53. W. Lee, M. K. Jin, W. C. Yoo and J. K. Lee, *Langmuir*, 2004, **20**, 7665–7669.
54. T.M. Galea, P. Attard, *Langmuir*, 2004, **20**, 3477–3482.
55. J. T. Chen, K. Shin, J. M. Leiston-Belanger, M. Zhang, T. P. Russell, *Adv. Funct. Mater.* 2006, **16**, 1476–1480.
56. Y.D He, H.J Qian, Z.Y Lu and Z.S Li, *Polym.* 2007, **48**, 3601–3606.
57. A. Jabbarzadeh, J.D. Atkinson, R.I. Tanner, *Phys. Rev.* 2000, **61**, 690–699.
58. W. Tian, K. L. Yung, Y. Xu, L. B. Huang, J. Kong and Y. C. Xie, *Nanoscale*, 2011, **3**, 4094–4100.
59. M. F. Zhang, P. Dobriyal, J. T. Chen, T. P. Russell, J. Olmo and A. Merry, *Nano Lett.*, 2006, **6**, 1075–1079.
60. W. Tian, Y. Xu, L.B. Huang, K.L. Yung, Y. Xie and W. Chen, *Nanoscale*, 2011, **3**, 5147–5155.
61. M. Steinhart, S. Murano, A.K. Schaper, T. Ogawa and M. Tsuji, *Adv. Funct. Mater.* 2005, **15**, 1656–1664.
62. M. Steinhart, J. H. Wendorff, A. Greiner, R. B. Wehrspohn, K. Nielsch, J. Schilling, J. Choi and U Gosele, *Science*, 2002, **296**, 1997.
63. W. Tian, X. D. Fan, J. Kong, T. Liu, Y. Y. Liu, Y. Huang, S. J. Wang and G. B. Zhang, *Macromolecules*, 2009, **42**, 640–651.
64. X. Chen, F. B. Surani, X. Kong, V. K. Punyamurtula, and Y. Qiao, *Appl. Phys. Lett.* 2006, **89**, 241918.
65. B. Xu, B. Wang, T. Park, Y. Qiao, Q. Zhou et al, *J. Chem. Phys.* 2012, **136**, 1847011.
66. L.B. Huang, Y. Zhou, S.T. Han, Y. Yan, L. Zhou and V.A.L. Roy, *Nanoscale*, 2014, **19**, 11013–11018
67. S.L Mei, X.D Feng and Z.X Jin, *Macromolecules*, 2011, **44**, 1615–1620.
68. H. W Fox, E.F Hare and W. A Zisman, *J. phys Chem*, 1995, **59**, 1097–1106.
69. M. Morita, T. Koga, H. Otsuka and A. Takahara, *Langmuir*, 2005, **21**, 911–918.
70. S.R. Carino, H. Tostmann, R.S. Underhill, J. Logan, G. Weerasekera and J. Culp, M David Son, R.S. Duran *J. Am. Chem. Soc.* 2001, **123**, 767–778.
71. J. Sagiv, *J. Am. Chem. Soc.* 1980, **102**, 92–98.
72. P.E. Laibinis and G.M. Whitesides, *J. Am. Chem. Soc.* 1992, **114**, 1990–1995.
73. C. I. Bouzigues, P. Tabeling and L. Bocquet, *Phys. Rev. Lett.* 2008, **101**, 114503.
74. P. Joseph, C. Cottin-Bizonne, J. M. Benoit, C. Ybert, C. Journet, P. Tabeling and L. Bocquet, *Phys. Rev. Lett.* 2006, **97**, 156104.
75. Y. X. Zhu and S. Granick, *Phys. Rev. Lett.* 2002, **88**, 106102.
76. Y. Li, J. Xu and D. Li, *Microfluid. Nanofluid.* 2010, **9**, 1011–1031.
77. K. Jayaraman, K. Okamoto, S.J. Son, C. Luckett, A.H. Gopalani and Lee S.B et al. *J. Am. Chem. Soc.* 2005, **127**, 17385–17392.
78. B.Y Cao, j. Kong, Y Xu, K.L. Yung and A Cai, *Heat. Transf. Eng.* 2013, **34**, 131–139.
79. P. Fontaine, M. Goldmann and F. Rondelez, *Langmuir*, 1999, **15**, 1348–1352.
80. T. Schmatko, H. Hervet and L. Leger, *Phys. Rev. Lett.* 2005, **94**, 244501.
81. B.D. Gates, Q.B Xu, M. Stewart, D. Ryan, C.G. Willson, and G.M. Whitesides, *Chem. Rev.* 2005, **105**, 1171–1196.
82. A.S.G. Curtis, B. Casey, J.O. Gallagher, D. Pasqui, M. A. Wood, and C. D. W. Wilkinson. *Biophys. Chem.* 2001, **94**, 275–283.
83. C. Vieu, F. Carcenac, A. Pepin, Y. Chen, M. Mejias, A. Lebib, L. Manin-Ferlazzo, L. Couraud, and H. Launois. *Appl. Surf. Sci.* 2000, **164**, 111–117.
84. A. Folch, A. Ayon, O. Hurtado, M. A. Schmidt, and M. Toner, *J. Biomech. Eng.* 1999, **121**, 28–34.
85. S. Affrossman, G. Henn, S.A. O'Neill, R.A. Pethrick, and M. Stamm, *Macromolecules*, 1996, **29**, 5010–5016.
86. S. Affrossman, S.A. O'Neill, and M. Stamm, *Macromolecules*, 1998, **31**, 6280–6288.
87. S. Affrossman, and M. Stamm, *Colloid. Polym. Sci.* 2000, **278**, 888–893.
88. S. Buttiglieri, D. Pasqui, M. Migliori, H. Johnstone, S. Affrossman, L. Sereni, M.L. Wratten, *Biomaterials*, 2003 **24**, 2731–2738.
89. M.J. Dalby, D. Giannaras, M.O. Riehle, N. Gadegaard, S. Affrossman, and A. S. G. Curtis, *Biomaterials*, 2004, **25**, 77–83.
90. M.A. Pattison, S. Wurster, T. J. Webster, and K. M. Haberstroh, *Biomaterials*, 2005, **26**, 2491–2500.
91. F.A. Denis, P. Hanarp, D. S. Sutherland, and Y. F. Dufrene. *Langmuir*, 2004, **20**, 9335–9339.
92. P. Hanarp, D.S. Sutherland, J. Gold, and B. Kasemo. *Colloids Surf. A Physicochem. Eng. Aspects*, 2003, **214**, 23–36.

93. A. Thapa, D. C. Miller, T.J. Webster, K.M. Haberstroh, *Biomaterials*, 2003, **24**, 2915–2926.
94. L. A. Smith, and P. X. Ma, *Colloids Surf.* 2004, **39**,125–131.
95. J. D. Hartgerink, E. Beniash, and S. I. Stupp. *Proc. Natl. Acad. Sci. USA*. 2002, **99**, 5133–5138.
96. T. Betancourt, L. Brannon-Peppas. *Intl J. Nanomedicine*, 2006, **1** 483–495.
97. H. Liu, S. H. Li, J. Zhai, H. J. Li, L. Jiang and D. B. Zhu, *Angew. Chem., Int. Ed*, 2004, **43**, 1146–1149.
98. M. Steinhart, B. R. Wehrspohn, U. Gsele, and J. H. Wendorff, *Chem. Int. Ed*, 2004, **43**, 1334 - 1344.
99. C. R. Martin, *Chem. Mater*, 1996, **8**, 1739-1746.
100. Y. Xu, W.Tian, W.Chen, K.L. Yung, L. B. Huang and C. L. Kang. *IEEE. Trans. Nanotechnol*, 2013, **12**, 659-661.
101. M. Steinhart, *Adv. Polym. Sci*, 2008, 123-187.
102. J. Martín, M. Vázquez, M. H. Vélez, and C. Mijangos, *J. Nanosci and Nanotechnol*, 2009, **9**, 5898-5902.
103. W. Lee, M. K. Jin, W. C. Yoo and J. K. Lee, *Langmuir*, 2004, **20**, 7665-7669.
104. P. Kohli, C.R. Martin, *J. Drug Deliv. Sci. Tech*. 2005, **15**, 49-57.
105. F. Buyukserin, P. Kohli, M.O. Wirtz, C.R. Martin, *Small*, 2007, **3**, 266-270.
106. L. Soleimany, A. Dolati and M. Ghorban, *J. Electroanalytical Chem* , 2010, **645** , 28-34.
107. CR. Martin, *Adv. Mater*, 1991, **3**, 457-459.
108. CR. Martin, *Acc. Chem. Res*, 1995, **28**, 61-68.
109. J. Martín, J. Maiz, J. Sacristan and C. Mijangos, *J. Polym.* , 2012, **53**, 1149-1166.
110. N. Valipour, J. Birjandi and Sargolzaei, *Physicochem. Eng. Aspects*, 2014, **448**, 93-106.
111. B. Sofia, and D. Mattia , *Colloid and Interface Sci.* 2011, **16**, 259-265.
112. A.V. Bazilevsky, K. Sun, A.L. Yarin and C.M. Megaridis, *J. Mater Chem*, 2008, **18**, 696-702.
113. M. Q. Tran, J. T. Cabral, M.S.P. Shaffer and A. Bismarck, *Nano. Lett.* 2008, **8**, 2744-2750.
114. A. Hirao and H. S. Yoo, *Polym. J.* 2011, **43**, 2-17.
115. W. L. Li, N.R. Tao and K. Lu, *Scripta Materialia*, 2008, **59**,546-549.
116. Kistler S.F, *Surfact. Sci.* 2005, **49**, 1988-1993.
117. H. Hillebrenner, F. Buyukserin, M. Kang, M. O. Mota, J. Stewar and C. R. Martin, *J. Am. Chem. Soc.* 2006, **128**, 4236-4237.
118. M. Steinhart, J.H. Wendorff and R.B. Wehrspohn, *Chem. Phys. Chem.* 2003, **4**, 1171-1176.
119. S. Dougherty and J. Liang, *Nanotechnology*, 2009, **20**, 295301.
120. M. Kokonou, G. Ioannou and C. Rebholz., *J.Nanopart Res.*2013, **15**, 1552.
121. A. Azarian, A. Irajizad, A. Dolati, S.M. Mahdavi, *Thin. Solid. Films*, 2009, **517**, 1736-1739.
122. S. Dougherty and J. Liang, *J.Nanopart Res*, 2009, **11**,743-747.
123. M. Bognitzkiet al, *Adv. Mater.* 2000,**12**, 637- 640.
124. D.X. Li, C.F. Li, A.H. Wang, Q. He, J.B. Li, *J. mater.chemi.* ,2010, **20**, 7782-7787.
125. N. Haberkorn, J.S. Gutmann and P. Theato, *ACS. Nano*, 2009, **3**, 1415-22.
126. A. Gitsas, B. Yameen, T.D. Lazzara, M. Steinhart, H. Duran and W. Knoll, *Nano.Lett*, 2010,**10**, 2173-2177.
127. B.Y. Cao, Y.W. Li, J. Kong, H. Chen, Y. Xu, K.L. Yung, A. Cai, *Polymer*, 2011, **52** , 1711-1715.
128. Y. Berdichevsky and Y.H. Lo, *Adv Mater*. 2006 **18**, 122-125.
129. S. Grimm, J. Martin, G. Rodriguez, M. Fernandez-Gutierrez, K. Mathwig, R.B. Wehrspohn, et al. *J Mater Chem*, 2010, **20**, 3171-3177.
130. Z. Hu, M. Tian, B. Nysten and A.M. Jonas., *Nature Materi.* 2009, **8** , 62-67.
131. L.F. Boesel, C. Greinerand, E. Arzt, *Adv. Mater.* 2010, **22**, 2125-2137.
132. Q. He, W. Song, H. Mohwald and J. Li , *Langmuir* ,2008a,**24**, 5508 -5513.
133. W.M. Lackowski, P. Ghosh, and R.M. Crooks, *J. Am .Chem. Soc.*, 1999,**121**, 1419 - 1420.
134. Q. He, Y. Tian, Y. Cui, H. Mohwald and J. Li, *J. Mater Chem.* 2008, **18**, 748-754.
135. Q. He, Y. Zhang, G. Lu, R. Miller, H. Mohwald and J. Li, *Adv. Colloid. Interf. Sci.* 2008c, **140**, 67-76.
136. D. R. Radu, C.Y. Lai, K. Jeftinija, E. W. Rowe, S. Jeftinija and V. Lin, *J.Am. Chem. Soc.* 2004, **126**, 13216-13217.
137. D. T. Mitchell, S. B. Lee, L. Trofin, , N. Li, T. K. Nevanen, H. Soderlund and C. R. Martin , *J. Am. Chem. Soc.* 2002, **124**, 11864-11865.
138. C. M. Sayes, R. Wahi, P. A. Kurian, Y. P. Liu, J. L. West, K. D. Ausman, D. B. Warheit and Colvin V. L., *Toxicol. Sci.* 2006, **92**, 174-185.
139. A.G. MacDiarmid, *Rev. Mod. Phys*, 2001, **73** , 701-713.
140. G. Cao and D. Liu, *Adv. Colloid. Interface. Sci.* 2008, **136**, 45-64.
141. R. Dersch , M. Steinhart , U. Boudriot , A. Greiner I and J. H. Wendorff I., *Polym. Adv. Technol*, 2005, **16**, 276-282.
142. H.C.Liao, P.C. Kuo, C.C.Lin, S.Y.Chen, *J. Vac. Sci. Technol., B* .2006, **24**, 2198.
143. H. Shin, D.K. Jeong, J. Lee, M. M. Sung, Kim, *J. Adv. Mater.* 2004,**16**, 1197-1200.
144. H.S. Woo, R. Czerw, S. Webster, D.L. Carroll, J. Ballato, A.E. Strevens and D. O'Brien, *Appl. Phys. Lett.* 2000, **77**, 1393-1395.
145. N. Valipour, F. Ch. Birjandi, J. Sargolzaei, *collid and surfaces physicochem. Eng. Asp.* 2014, **448**, 93-106.
146. S.M. Sedghi, D. Rodrigue, J.Brisson, M.C. Iliuta, *j memb, sci*, 2014, **452**, 332-353.
147. J. P. Cannon, S. D. Bearden, S.A. Gold, *synthe metal*, 2010, **160**, 2623-2627.
148. M. C. Serrano, M. C. Gutiérrez, F. D Monte, *prog. Polym. Sci.* 2014 in press.
149. T.M. Galea and P. Attard, *Langmuir*, 2004, **20**, 3477-3482.
150. J. Kong, Y. Xu , K.L.Yung, Y. Xie and L. He, *J. Phys. Chem.C.* 2009, **113**, 624-629.
151. Y.Wang, S.Shimada, Y.Yamamoto, N. Miyaura , *Mater. Res.Bull.* 2008, **43**, 251-256.